Bifurcations in the quantum nonlinear dimer

V. M. Kenkre
Department of Physics and Astronomy, University of New Mexico, Albuquerque, New Mexico 87131

Marek Kuś
Centrum Fizyki Teoretycznej, Polska Akademia Nauk, al. Lotników 32/46, 02-668 Warszawa, Poland
(Received 29 July 1993)

Strong interactions with phonons cause nonlinearity to appear in the evolution of quasiparticles such as electrons, or electronic and vibrational excitations. Our study of the evolution of such nonlinear quantum systems, when they are placed in contact with a thermal reservoir, has been found to exhibit rich behavior including a Hopf bifurcation. The nature of this bifurcation is studied and experimental manifestations are indicated.

I. INTRODUCTION

The purpose of this paper is to report some interesting behavior we have observed in a simple model that has recently undergone intense analysis. The model is the quantum nonlinear dimer.[1–4] It represents a quasiparticle such as an electron or an electronic or vibrational excitation ringing back and forth between two states, such as two sites on a molecule, while interacting strongly with vibrations. The interaction with vibrations is strong enough to introduce nonlinearity in the motion of the quasiparticle, the nonlinearity being particular to equations such as the discrete nonlinear Schrödinger equation[5] (DNLSE) and to objects such as the soliton or the polaron.[6] The two-site system (dimer) has intrinsic interest both because it is an often tractable representation of more complicated spatially extended systems and because it corresponds directly to several experimentally realizable objects.[1,3,7,8]

The striking observation that we report in this paper is the appearance of a Hopf bifurcation in its evolution. The equations of motion which result in this interesting behavior were derived by Kenkre and Grigolini[9] via a Fokker-Planck method followed by a contraction procedure to obtain closed evolution equations for average quantities,

$$\frac{dp}{dt} = q, \tag{1.1a}$$

$$\frac{dq}{dt} = -p - \chi pr + \frac{\chi}{\Gamma} qr - \alpha q, \tag{1.1b}$$

$$\frac{dr}{dt} = \chi pq - \frac{\chi}{\Gamma} q^2 - \alpha(r - r_{\rm eq}), \tag{1.1c}$$

where p, q, and r are ensemble averages, i.e., mixed-state counterparts of the respective pure-state quantities

$$p' = |c_1|^2 - |c_2|^2, \quad q' = i(c_1 c_2^* - c_2 c_1^*),$$
$$r' = c_1 c_2^* + c_2 c_1^*, \tag{1.2}$$

and c_1 and c_2 are the probability amplitudes for the particle being at sites 1 and 2, respectively. Equations (1.2) will form the point of departure of the analysis in the present paper. We refer the reader to Ref. 9 for the details of their derivation but point out here that they arise from the following coupled Schrödinger equations describing the evolution of the amplitudes c_1 and c_2 at sites 1 and 2 coupled to the vibrational modes x_1 and x_2,

$$\frac{idc_1}{dt} = Vc_2 + Ex_1 c_1, \tag{1.3a}$$

$$\frac{idc_2}{dt} = Vc_1 + Ex_2 c_2, \tag{1.3b}$$

where V is the intersite transfer matrix element of the quasiparticle and E characterizes the coupling between the quasiparticle and the vibrations. The dynamics of the vibrational modes is given by

$$\frac{d^2 x_m}{dt^2} + \omega^2 x_m = -(\text{const})|c_m|^2, \quad m = 1, 2. \tag{1.4}$$

The right hand side of the above equation describes the strong interaction between the quasiparticle and the lattice vibration which shifts the equilibrium position of the oscillator by the amount proportional to the probability of occupation of the state by the quasiparticle. The introduction of dissipation, the incorporation the thermal bath via standard techniques, and the elimination of the vibrational degrees of freedom in the limit of high damping lead to the following equation for the probability distribution $\sigma(p, q, r; t)$:[9]

$$\frac{\partial \sigma(p,q,r;t)}{\partial t} = L\sigma(p,q,r;t), \tag{1.5}$$

with

$$L = 2V\left(p\frac{\partial}{\partial q} - q\frac{\partial}{\partial p}\right) + \chi p\left(r\frac{\partial}{\partial q} - q\frac{\partial}{\partial r}\right) + \frac{2V}{\Gamma}\chi\, q\left(q\frac{\partial}{\partial r} - r\frac{\partial}{\partial q}\right) + \frac{2\chi k_B T}{\Gamma}\left(r^2\frac{\partial^2}{\partial q^2} - \frac{\partial}{\partial q}r\frac{\partial}{\partial r}q - \frac{\partial}{\partial r}q\frac{\partial}{\partial r}r + q^2\frac{\partial^2}{\partial q^2}\right). \tag{1.6}$$

The exact consequence of (1.6) is the following set of coupled equations for the thermal averages of the variables p, q, r and their higher moments:

$$\frac{d\langle p\rangle}{dt} = 2V\langle q\rangle, \tag{1.7a}$$

$$\frac{d\langle q\rangle}{dt} = -2V\langle p\rangle - \chi\langle pr\rangle + \frac{2V\chi}{\Gamma}\langle qr\rangle - \alpha\langle q\rangle, \tag{1.7b}$$

$$\frac{d\langle r\rangle}{dt} = \chi\langle pq\rangle - \frac{2V\chi}{\Gamma}\langle q^2\rangle - \alpha\langle r\rangle. \tag{1.7c}$$

A contraction procedure and the use of the explicit expression for the stationary solution of the Fokker-Planck equation (1.5) finally lead to Eqs. (1.2) which form our starting point.

The equilibrium value r_{eq}, which is the difference in probabilities of occupation of the two quantum states accessible to the system, should be generally given as[10]

$$r_{eq} = \tanh\left(\frac{V}{k_BT}\right) = \tanh\left(\frac{\chi}{\Gamma\alpha}\right). \tag{1.8}$$

The last equality is based on an approximate description[9] for α, viz.,

$$\alpha = \frac{\chi k_BT}{\Gamma V}. \tag{1.9}$$

The system (1.1) reduces to the one describing the trivial linear dimer if $\chi = 0 = \alpha$, to the high-temperature damped linear dimer if χ vanishes but α does not, to the nonlinear adiabatic dimer if χ is finite but Γ infinite and α vanishes,[1–3] to a relatively crude extension[11] of the nonlinear dimer to dissipative situations if χ is finite, Γ infinite and r_{eq} vanishes, and to the nonlinear nonadiabatic dimer if χ and Γ are finite and α vanishes.[12]

II. NUMERICAL INVESTIGATIONS OF EVOLUTION

A study of Eqs. (1.1) through numerical integration uncovers a multitude of phenomena. Consider the case when the quasiparticle occupies one of the two states initially. For vanishing α, the probability difference oscillates and then tends to the stationary value which is zero if the nonlinearity parameter is small enough, and finite (corresponding to a localized state) if it is large enough. In the latter case, as α increases, the detrapping effect is seen: p tends to zero at larger times even for large nonlinearities [Fig. 1(a)]. In addition to these earlier findings,[9] we find that, as α increases further, a surprising bursts of p occurs for a short time, recurring after a time period [Figs. 1(b,c)]. The bursts become more frequent with further increase of α and behavior that *appears* chaotic occurs. Plots of the time dependence of r depict related behavior. For larger values of α, after some time, a limit cycle behavior has been reached: p, q, and r oscillate steadily (Figs. 2). A further increase in α destroys the

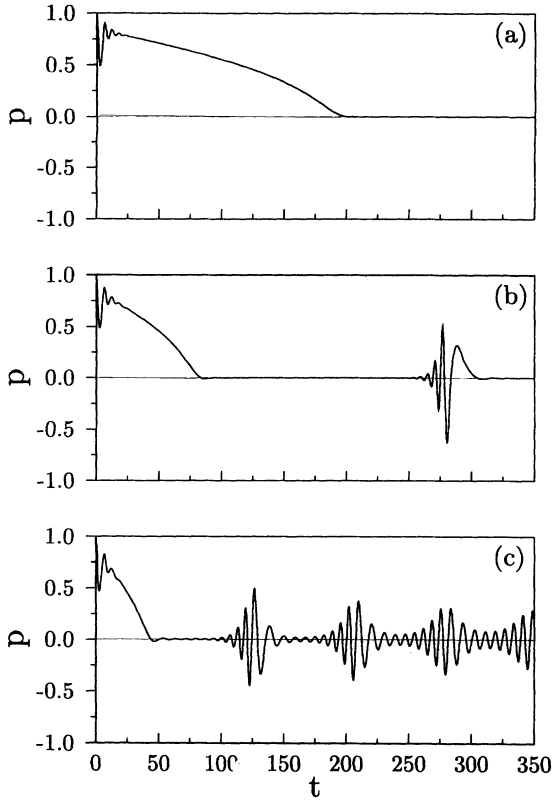

FIG. 1. Time evolution of p the difference between occupation probabilities of the two sites for $\chi = 1 = \Gamma$. (a) $\alpha = 0.002$, (b) $\alpha = 0.005$, (c) $\alpha = 0.01$.

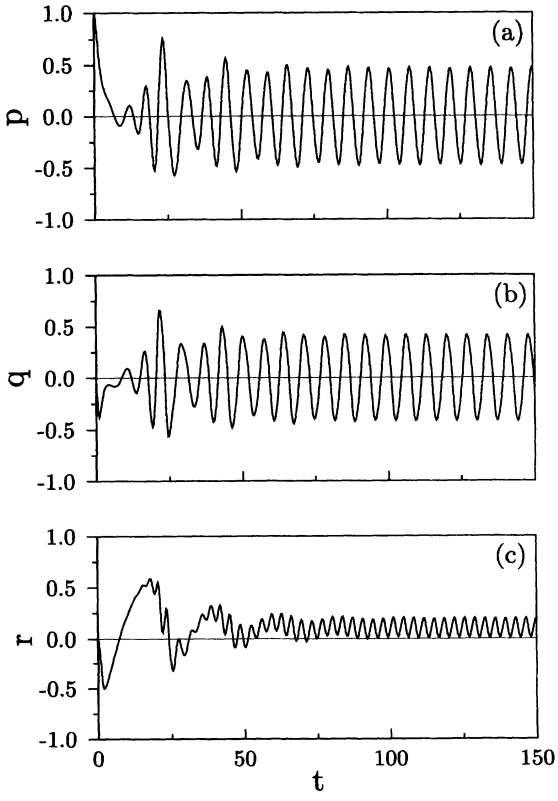

FIG. 2. Time evolution of the variables p, q, and r, respectively in (a), (b), and (c) for $\chi = 1 = \Gamma$ and $\alpha = 0.33$.

limit cycle, and stable dissipative behavior is met, as p and q tend to vanishing values while r tends to r_{eq} (Figs. 3 and 4).

The reason for the rich behavior that emerges from Eqs. (1.1) when r_{eq} is taken to be nonzero is quite simple: This term serves as a driving agent in the nonlinear system. Interplay between temperature-dependent driving and temperature-dependent dissipation lead then to the observed phenomena. A full analysis is given in the next section.

III. BIFURCATIONS OF STEADY STATE SOLUTIONS

The set of nonlinear equations (1.1) has the unique stationary solution

$$p_0 = 0, \quad q_0 = 0, \quad r_0 = r_{eq}. \tag{3.1}$$

The character of this solution (its stability) depends on the values of the relevant parameters α, χ, Γ, and r_{eq}. To analyze the stability, we simply investigate trajectories starting from the points close to the stationary solution, so close, that we can linearize the system. The resulting equations, being linear, are easy to investigate: If the eigenvalues of the linear problem all have negative real parts, points initially close to the stationary solution evolve towards it—the stationary solution is stable. Linearizing the equations around the stationary solution, we find that the eigenvalues of the linearization matrix are

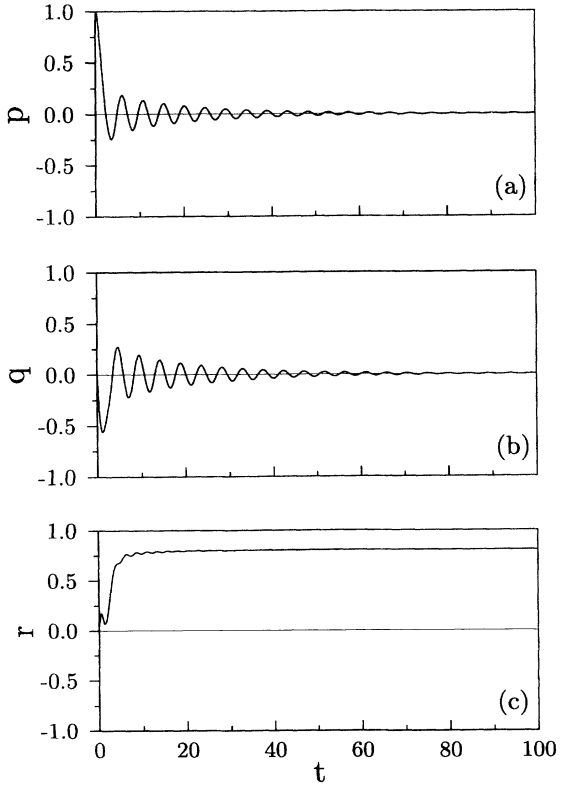

FIG. 3. Same as Fig. 2 but for $\alpha = 0.9$.

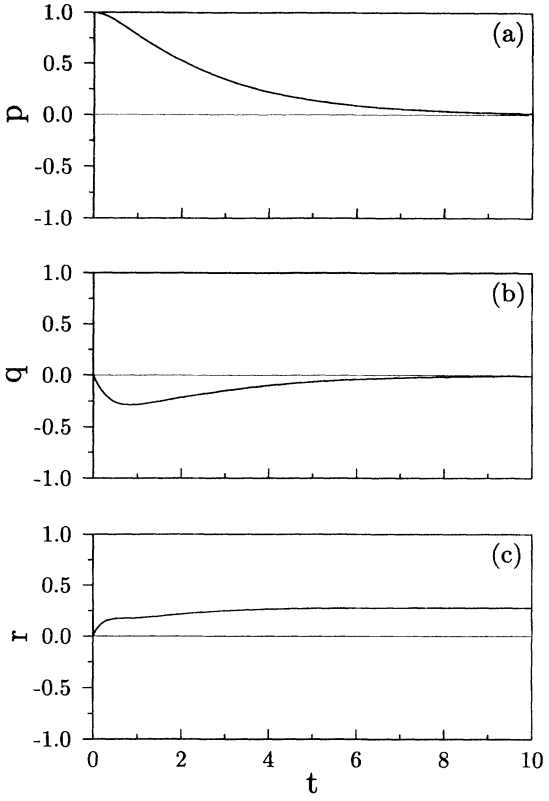

FIG. 4. Same as Fig. 2 but for $\alpha = 3.5$.

given by

$$\lambda_{1,2} = \frac{1}{2}\left[\frac{\chi}{\Gamma}r_{eq} - \alpha \pm \sqrt{\left(\frac{\chi}{\Gamma}r_{eq} - \alpha\right)^2 - 4(1+\chi r_{eq})}\right], \tag{3.2a}$$

$$\lambda_3 = -\alpha. \tag{3.2b}$$

Equation (3.2) show that the stationary solution is stable for sufficiently large values of the damping α, when the dissipation is large enough to overtake the influence of the thermal driving proportional to r_{eq}. From the explicit formulas given above, we find this condition to be

$$\alpha > \frac{\chi}{\Gamma}r_{eq}. \tag{3.3}$$

We thus see that there is a critical demarcation value of α which separates stable from unstable regions.

Imaginary parts of the pair of the eigenvalues λ_1, λ_2 determine the way the equilibrium position is approached. If the imaginary parts vanish, which is the case for large enough α,

$$\alpha > \frac{\chi}{\Gamma}r_{eq} + 2(1+\chi r_{eq})^{1/2}, \tag{3.4}$$

the approach of the p and q variables to their equilibrium value is monotonic (for large time) as illustrated in Fig. 4 where the time evolution of the variables p, q, and r is

shown. Phase space trajectory, projected on the p-q and p-r planes, is presented in Fig. 5(a).

For

$$\frac{\chi}{\Gamma}r_{\rm eq} + 2(1+\chi r_{\rm eq})^{1/2} > \alpha > \frac{\chi}{\Gamma}r_{\rm eq}, \tag{3.5}$$

the real parts of $\lambda_{1,2}$ are still negative, but their imaginary parts do not vanish any longer and the motion toward the equilibrium takes a spiraling form in the p-q plane [Fig. 5(b)]. The time evolution of each of these variables exhibits oscillations before settling down to the zero equilibrium value (see Fig. 3). The third eigenvalue λ_3, which governs the rate of equilibration of the variable r to its stationary value $r_{\rm eq}$, is always real (and negative). As a result approach of the equilibrium along this direction is monotonic (after large enough time).

At $\alpha = \alpha_H = \chi r_{\rm eq}/\Gamma$ the stationary solution loses its stability (the real part of $\lambda_{1,2}$ eigenvalues becomes zero and positive for even smaller values of α). The interplay between dissipation (characterized by α) and thermal excitation (measured by $r_{\rm eq}$) becomes more subtle. The excitation is strong enough to sustain oscillations in the system with nondiminishing amplitude. The equilibrium solution bifurcates to a periodic solution (Hopf bifurcation). The stability of the periodic solution can be also investigated by analyzing behavior of neighboring trajectories. Technically, such an analysis is more complicated than that of the stability of stationary solutions, but conceptually it consists also in a linearization of the system in the vicinity of the periodic trajectory. It can be proved, using the algorithm given in Ref. 13, that the Hopf bifurcation leads in our case to the emergence of a *stable* limit cycle, which attracts neighboring trajectories as illustrated in Fig. 5(c). Observe that, due to the fact that the rate of dissipation α becomes smaller when going from Fig. 4 through Fig. 3 to Fig. 2, the actual time after which the system reaches its equilibrium state (stationary as in Figs. 4 and 3 or an oscillatory one as in Fig. 2) is longer and longer.

According to the general theory of the Hopf bifurcation, for values of α not far from the bifurcation value α_H the amplitude of the oscillations grows as $\sqrt{\alpha - \alpha_H}$ when α departs from its bifurcation value α_H, whereas the frequency of the revolution along the closed orbit is approximately given by the value of the imaginary part of the eigenvalues $\lambda_{1,2}$ at the bifurcation point α_H.[13] As α goes farther and farther from the bifurcation value, nonlinear effects start to play more important role and the amplitude starts to shrink after taking the maximum value at (approximately) $\alpha = 0.33$. The dependence of the limiting closed orbit on the value of α is illustrated in Fig. 6. We plotted here the values of the variables p, q, and r only for times long enough to reach the orbit, skipping the initial approach to it. The plots show p-q and p-r projections of the orbit.

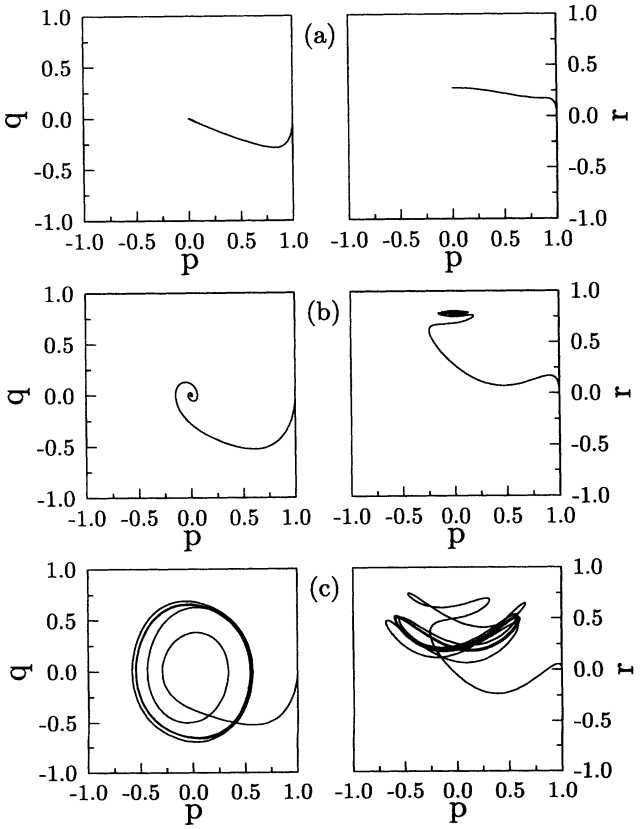

FIG. 5. Phase space plots of the trajectory in the p-q and p-r planes for $\chi = 1 = \Gamma$. (a) $\alpha = 0.33$, (b) $\alpha = 0.9$, (c) $\alpha = 3.5$.

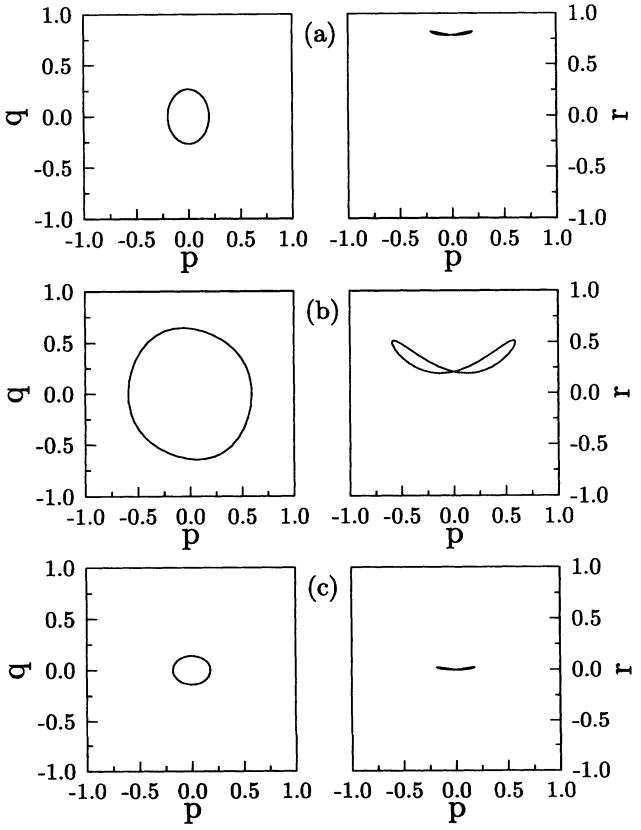

FIG. 6. Trajectories in the p-q and p-r planes for times long enough for the system to reach the limit cycle. (a) $\alpha = 0.8$, (b) $\alpha = 0.33$, (c) $\alpha = 0.01$. In all three cases $\chi = 1 = \Gamma$.

The long time evolution of the variables for $\alpha = 0.33$ is shown in Fig. 7. The regular oscillatory patterns suggest a simple analytic approximation to the real evolution *on* the limit orbit (i.e., after reaching it), consisting of taking into account only the lowest harmonics of the periodic motion. Indeed postulating

$$p = p_H \cos(\omega t), \tag{3.6a}$$
$$q = q_H \sin(\omega t), \tag{3.6b}$$
$$r = r_1 \sin(2\omega t) + r_2 \cos(2\omega t) + r_3, \tag{3.6c}$$

substituting this to the original nonlinear system of equations, neglecting higher harmonics, and comparing the coefficients of $\sin(\omega t), \cos(\omega t), \sin(2\omega t), \cos(2\omega t)$, and the constant terms, we arrive at a nonlinear algebraic system of equations for p_H, q_H, r_1, r_2, r_3 which can be solved in the form

$$p_H = \frac{1}{\omega}\sqrt{\frac{-2\Gamma}{\chi}}C, \tag{3.7a}$$
$$q_H = -\omega p_H, \tag{3.7b}$$
$$r_1 = \frac{\alpha}{\alpha^2 + 4\omega^2}\left(\frac{\alpha\Gamma\rho}{\omega} - 2\omega\right)C, \tag{3.7c}$$
$$r_2 = \frac{\alpha}{\alpha^2 + 4\omega^2}(\alpha - 2\Gamma\rho)\,C, \tag{3.7d}$$
$$r_3 = C + r_{\rm eq}, \tag{3.7e}$$

with

$$C = \frac{(\omega^2 - \rho^2)(4\omega^2 + \alpha^2)}{\chi(4\rho - \Gamma\alpha) + \chi\alpha(1 + \chi r_{\rm eq})(\alpha - \Gamma)} \tag{3.8}$$

and

$$\rho = \sqrt{1 + \chi r_{\rm eq}}. \tag{3.9}$$

The frequency ω is a solution of the equation

$$4\omega^6 + \left[\frac{3}{2}\alpha^2 - 4\rho^2 + (4\Gamma - \alpha)\left(\frac{\chi}{\Gamma}r_{\rm eq} - \alpha\right)\right]\omega^4 + \left[\frac{\Gamma^2\alpha^2\rho^2}{2} - \frac{3}{2}\alpha^2\rho^2 + \Gamma\alpha\rho(\alpha - \Gamma\rho)\left(\frac{\chi}{\Gamma}r_{\rm eq} - \alpha\right)\right]\omega^2 - \frac{\Gamma^2\alpha^2\rho^4}{2} = 0. \tag{3.10}$$

Observe that, at the bifurcation point, i.e., for $\alpha = \alpha_H = \chi r_{\rm eq}/\Gamma$, the above equation reduces to

$$(\omega^2 - \rho^2)\left(4\omega^4 + \frac{3}{2}\alpha^2\rho^2\omega^2 + \frac{\Gamma^2\alpha^2\rho^2}{2}\right) = 0. \tag{3.11}$$

One of the solutions of Eq. (3.11) is $\rho = \sqrt{1 + \chi r_{\rm eq}}$, which is the imaginary part of the eigenvalue $\lambda_{1,2}$ at the bifurcation point in accordance with the general theory of the Hopf bifurcation. Continuation of this particular branch of solution of the Eq. (3.10) for $\alpha < \alpha_H$ gives the desired approximation. Moreover, a simple calculation shows that the amplitudes of the neglected higher harmonics are indeed small when compared with p_H, q_H, r_1, r_2, and thus reassures us that the procedure is self-consistent. The quality of the described approximation is illustrated in Fig. 8 where the exact numerical solution of the system is compared with our approximation. The figure corresponds to the value of $\alpha = 0.33$, which gives the maximal amplitude of the oscillations. Further numerical investigations have shown that this value corresponds to what is actually the worst approximation. The accuracy of our approximation is, therefore, rather satisfactory as is visually obvious from Fig. 8.

Further numerical investigation show that, when the dissipation parameter α is diminished further, the amplitude of the oscillation is also diminished, but that the limiting stable orbits persists. As α tends to zero, the os-

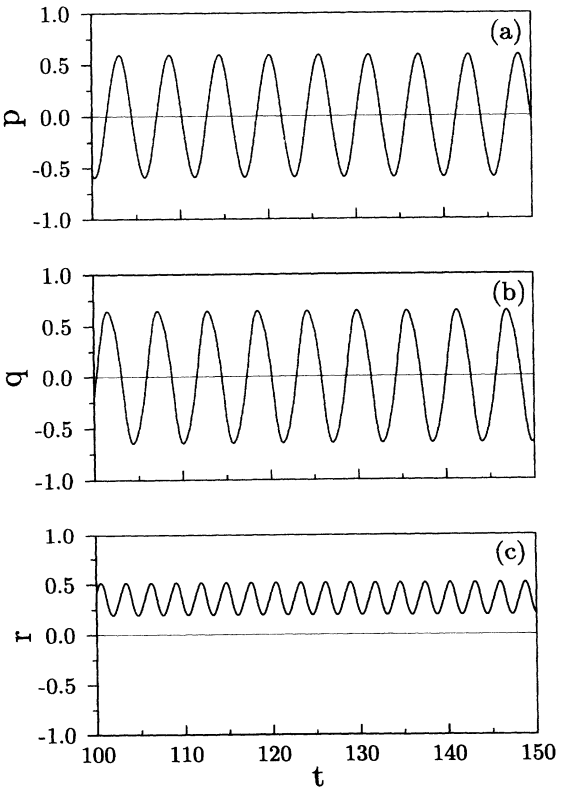

FIG. 7. Long-time evolution of the variables p, q, and r, respectively in (a), (b), and (c) for $\chi = 1 = \Gamma$ and $\alpha = 0.33$.

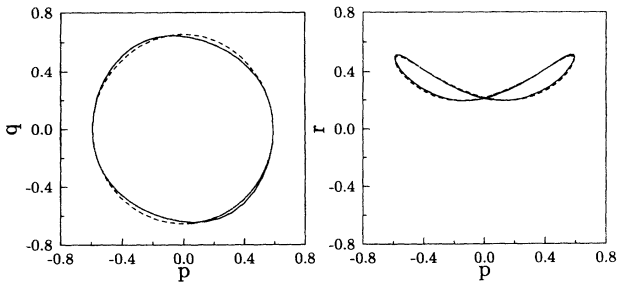

FIG. 8. Comparison between exact (solid line) and approximate (dashed line) limit-cycle trajectories for $\alpha = 0.33$, $\chi = 1 = \Gamma$.

cillation amplitude also tends to zero, but equilibration takes forbiddingly long time to complete. The evolution of the system is dominated by transients during which trajectories explore various regions of the configuration space of the variables p, q, r. This exploration, from time to time, takes form of sudden "bursts" separated by more "laminar" phases.

IV. CONCLUDING REMARKS

As we have seen above, despite its apparent simplicity, the quantum nonlinear dimer contains a multitude of interesting physics, particularly when it is in interaction with a thermal reservoir. The starting point of our analysis in the present paper has been the coupled equations of motion (1.1) derived by Kenkre and Grigolini[9] on the basis of a Brownian motion treatment of the quantum nonlinear dimer. It has been suggested[4] that the equation appear to be reasonable and capable of unifying various tendencies of the nonlinear dimer in different parameter regimes. Since a completely rigorous justification of the truncation of the coupled hierarchy (1.7) is not available, it is not inconceivable that Eqs. (1.1) are inaccurate. However, the derivation and examination of the range of validity of Eqs. (1.1) are not the subject matter of the present paper. We have been interested here only in exploring their consequences.

These consequences have been found to be exciting, particularly in that they involve bifurcation behavior. We have shown the bifurcation to be of the Hopf kind. As shown by Eq. (1.9) variations of the rate α are connected simply to temperature variations. Bifurcations correspond, therefore, to specific temperature values, and the interesting behavior depicted in Figs. 6 and 7 can be accessed, in principle, by simply changing the temperature.

The rich low-temperature behavior noted in Secs. II and III would be reflected in a number of experimental observables. Here we merely indicate that fluorescence depolarization of stick dimers would be one of the more convenient observational setups to test our findings. While we refer the reader to Ref. 1 for details, we point out here that the crucial quantity is the fluorescence depolarization ratio f given by the ratio of the difference and the sum of intensities of emitted light with polarization direction respectively parallel and perpendicular to that of the incident light. This quantity is given by[1]

$$f(t) = p(t)\cos 2\phi + r(t)\sin 2\phi, \tag{4.1}$$

where ϕ is the angle made by the polarization of the incident light with the induced dipole moment on one of the two molecules forming the dimer. The angle ϕ is controllable. The bifurcation behavior present in $p(t)$ and $r(t)$ will thus be directly reflected in behavior of the experimental observable $f(t)$. For the values of α above the bifurcation value, when $p(t)$ and $r(t)$ tend to constant stationary values, $f(t)$ will also tend to its final asymptotic (constant) value, whereas for α below the bifurcation value, in accord with Eqs. (3.6) and (4.1), $f(t)$ will ultimately reach a periodic regime dominated by the frequency ω given by Eq. (3.10). We hope that the analysis presented here will stimulate experimental efforts which could uncover the rich bifurcation behavior that appears to present even in simple quantum nonlinear systems.

ACKNOWLEDGMENT

M.K. was partially supported by Polish KBN Grant No. 2 P302 092 05.

[1] V. M. Kenkre, in *Singular Behaviour and Nonlinear Dynamics*, edited by S. Pnevmatikos, T. Bountis, and S. Pnevmatikos (World Scientific, Singapore, 1989), Vol. II, and references therein.

[2] J. Eilbeck, P. S. Lomdahl, and A. C. Scott, Physica D **16**, 318 (1985).

[3] V. M. Kenkre and D. K. Campbell, Phys. Rev. B **34**, 4959 (1986); V. M. Kenkre and G. P. Tsironis, *ibid.* **35**, 1473 (1987).

[4] V. M. Kenkre, in *Future Directions in Nonlinear Sciences in Physics and Biology*, edited by J. C. Eilbeck, P. L. Christiansen, and R. Parmentier (Plenum, New York, 1993).

[5] *Davydov's Soliton Revisited*, edited by P. L. Christiansen and A. C. Scott (Plenum, New York 1990).

[6] A. C. Scott, Phys. Rep. **217**, 1 (1992).

[7] V. M. Kenkre and G. P. Tsironis, Chem. Phys. **128**, 219 (1988).

[8] T. S. Rahman, R. S. Knox, and V. M. Kenkre, Chem. Phys. **44**, 197 (1979).

[9] V. M. Kenkre and P. Grigolini, Z. Phys. B **90**, 247 (1993); for the basic formalism see also P. Grigolini, H.-L. Wu, and V. M. Kenkre, Phys. Rev. B **40**, 7045 (1989).

[10] See, e.g., R. K. Pathria, *Statistical Mechanics* (Pergamon Press, Oxford, 1972).

[11] G. P. Tsironis, V. M. Kenkre, and D. Finley, Phys. Rev. A **37**, 4474 (1989).

[12] V. M. Kenkre and H.-L. Wu, Phys. Rev. B **39**, 6907 (1989); Phys. Lett. A **135**, 120 (1989).

[13] J. E. Marsden and M. McCracken, *The Hopf Bifurcation and Its Applications* (Springer, New York, 1976).